

Population Pharmacokinetics of Phosphocreatine and its metabolite Creatine in Children with Myocarditis

Huan He¹, Meng Zhang², Li-Bo Zhao², Ning Sun², Yi Zhang², Yue Yuan², and Xiaoling Wang²

¹Beijing Children's Hospital, Capital Medical University, National Center for Children's Health, Beijing 10045, China

²Affiliation not available

May 20, 2020

Abstract

Aims This study aimed to develop a parent-metabolite joint population pharmacokinetic model to characterize the pharmacokinetic (PK) profile for phosphocreatine (PCr) and its metabolite creatine (Cr) in children with myocarditis, and to use this model to study the PK profile of different dosing schemes. **Methods** One hundred pediatric patients with myocarditis were enrolled. Blood samples were collected at baseline and, approximately 30, 40 or 50, 75 and 180 min after a single dose of phosphocreatine sodium. Plasma PCr and Cr concentrations were determined using a HPLC-MS/MS method. A nonlinear mixed-effects model approach was used to build the population pharmacokinetic model. After validation, the model was used for simulations to evaluate the PK profile of different dosing schemes. **Results** A total of 997 plasma concentrations (498 for PCr and 499 for Cr) were included in the analysis. A four-compartment chain model (central and peripheral compartments for both PCr and Cr) with first-order elimination adequately characterized the in vivo process of PCr and Cr. Allometric scaling based on bodyweight was applied to the PK parameters. The covariate analysis identified that the glomerular filtration rate (GFR) was strongly associated with the Cr clearance. Bootstrap and visual predictive check suggested a robust and reliable pharmacokinetic model was developed. The simulation results showed that the PCr had no accumulation in vivo. With the infusion of PCr, the concentration of Cr increased rapidly. **Conclusion** The joint population pharmacokinetic model for PCr and Cr in pediatric patients with myocarditis was successfully developed for the first time.

Methods

One hundred pediatric patients with myocarditis were enrolled. Blood samples were collected at baseline and, approximately 30, 40 or 50, 75 and 180 min after a single dose of phosphocreatine sodium. Plasma PCr and Cr concentrations were determined using a HPLC-MS/MS method. A nonlinear mixed-effects model approach was used to build the population pharmacokinetic model. After validation, the model was used for simulations to evaluate the PK profile of different dosing schemes.

Results

A total of 997 plasma concentrations (498 for PCr and 499 for Cr) were included in the analysis. A four-compartment chain model (central and peripheral compartments for both PCr and Cr) with first-order elimination adequately characterized the in vivo process of PCr and Cr. Allometric scaling based on bodyweight was applied to the PK parameters. The covariate analysis identified that the glomerular filtration rate (GFR) was strongly associated with the Cr clearance. Bootstrap and visual predictive check suggested a robust and reliable pharmacokinetic model was developed. The simulation results showed that the PCr had no accumulation in vivo. With the infusion of PCr, the concentration of Cr increased rapidly.

Conclusion

The joint population pharmacokinetic model for PCr and Cr in pediatric patients with myocarditis was successfully developed for the first time.

What is already known about this subject

- Exogenous PCr is believed to participate in energy metabolism in damaged myocardium and it has been used as cardio-protective drug and applied to the therapy of myocarditis.
- The pharmacokinetics of PCr in adults and animals has been studied, however the available information about PCr in children was limited.

What this study adds

- To our knowledge, this is the first PK study of PCr in children.
- We developed a comprehensive population pharmacokinetic model of PCr and its metabolite Cr for the first time.
- The PCr had no accumulation in vivo after multiple dosing and with the infusion of PCr, the concentration of Cr increased rapidly.

Introduction

Pediatric myocarditis is a common disease of cardiovascular system in children [1]. It has become a serious threat to the life and health of children owing to its complex clinical manifestations, rapidly illness development and lacking of specificity diagnosis methods [2].

Phosphocreatine (PCr) is an important endogenic high-energy phosphate compound in the human or mammalian animals. It acts as a crucial part in cellular energy metabolism by acting as an immediately temporal and spatial energy buffer for the intracellular energy transport [3, 4]. PCr was metabolized into creatine (Cr) and generate ATP by creatine kinase [5]. ATP consumption during myocardial injury is mainly replenished by PCr transformation. At present, PCr could be obtained by artificial synthesis. Exogenous complementary PCr is believed to help solve the most fundamental problem of energy metabolism in damaged myocardium and it has been used as a cardio-protective drug and applied to the therapy of heart failure or myocardial infarction [6-9].

Exogenous PCr also has begun to be used in the therapy of pediatric myocarditis [2]. In addition, it has also been recorded in the Chinese National Formulary (page 212, the chemical and biological products for children) and the Chinese Pharmacopoeia (2015), as the drug for viral myocarditis. The pharmacokinetics (PK) of PCr in adults and animals has already been studied [10-12]. After intravenous PCr in mice, the changes of PCr concentrations were consistent with two-compartment model and most of PCr are metabolized to Cr [10]. The PK studies of PCr in adults also showed that the elimination of PCr in human body was two-phase elimination [11]. While, the distribution of its major metabolite Cr in human body has not been studied.

However, the currently available information about PCr in children was limited which was considered as “off-label use”. The PK of PCr and Cr in children is unknown and interindividual variability (IIV) is not clear.

To resolve the above problems, the population pharmacokinetics of PCr and its metabolite Cr in Chinese children was performed at Beijing Children’s Hospital. This study was designed to understand the pharmacokinetic behavior of PCr and Cr in children after intravenous infusion and identify significant factors influencing PK parameters, so as to provide evidence for rational use in children.

Methods

Subject selection

This study was conducted at Beijing Children’s Hospital, Capital Medical University. Inclusion criteria were (1) age less than 18 years old, (2) boys or girls, (3) clinically diagnosed pediatric myocarditis and (4) the acute stage in the clinical stage of myocarditis. The main exclusion criteria were as follows: allergy to Phosphocreatine Sodium, other causes of myocardial injury, a history of heart disease, other serious illnesses, other causes of electrocardiogram changes, participated in other clinical trials prior to screening and patients with renal insufficiency. The baseline information included gender, age (year), height (cm), bodyweight (BW, kg), disease duration, white blood cell count (WBC), red blood cell count (RBC), hemoglobin (HGB), blood platelet count (PLT), percentage of neutrophils (NEUT), lymphocyte percentage (LYMPH), percentage of monocytes (MONO), percentage of eosinophilic cells (EO), percentage of basophilic cells (BASO), total protein (TP), albumin (ALB), alkaline phosphatase (ALP), aspartate transaminase (AST), alanine transaminase (ALT), total bilirubin (TBIL), direct bilirubin (DBIL), urea, creatinine, uric acid (UA), creatine kinase (CK), creatine kinase-MB (CK-MB), lactic dehydrogenase (LDH), alpha-hydroxybutyric dehydrogenase (HBDH) and hypersensitive troponin -I (HSTN-I). The details of these clinical data characteristics are provided in the Supplemental Material 1. The glomerular filtration rate (GFR) for children older than 1 and younger than 18 was calculated using the creatinine-based “Bedside Schwartz” equation (currently considered the best method for estimating GFR in children) [13]. For children under 1 year old, the GFR was estimated using the original Schwartz equation [14]. This clinical trial protocol was approved by the Ethics Committee of Beijing Children’s Hospital (Approval number: [2016]-Y-013-C-02). Written informed consent was obtained from each enrolled patient or their legally authorized guardian.

Study design

Participants received a single intravenous infusion of phosphocreatine sodium according to their age (28 days \sim < 1 year old: 0.5 g, 1 \sim < 6 years old: 1 g, 6 \sim < 18 years old: 2 g). The above phosphocreatine sodium was dissolved in 50 ml 0.9% sodium chloride injection and continuously injected with an intravenous pump within 30 ± 2 min. Blood samples from the arm without an intravenous infusion were collected at baseline (before infusion) and, approximately 30, 40 or 50, 75 and 180 min after the start of infusion. The actual infusion time and sampling time were recorded. The blood samples were centrifuged at 4°C (3000 rpm) for 10 min, and the plasma at upper layer was separated and stored immediately at -40°C until analysis.

Sample assay

An improved HPLC-MS/MS method based previous literature [15] was used to measure plasma concentrations of PCr and Cr, using salidroside and creatine-(methly-d3) (Cr-d3) as internal standards, respectively. 50 μ L of plasma and 10 μ L of internal standard solution (20 μ g/mL salidroside and 100 μ g/mL Cr-d3 for PCr and Cr determination, respectively) were prepared by protein precipitation with acetonitrile/water (1000 μ L, 1:1, v/v). After vortex and centrifugation, 100 μ L of the supernatant fluid was diluted with 500 μ L of solvent, and 10 μ L was injected into the HPLC-MS/MS system for the determination of PCr. While, for the Cr determination, 20 μ L of the supernatant fluid was diluted with 1000 μ L of solvent, and 5 μ L was injected into the HPLC-MS/MS system.

A Hypersil Gold C₁₈ column (150×2.1 mm, 5 μ m, Thermo Scientific, USA) was used for separation of PCr. The mobile phase was solution A: 2 mM ammonium acetate in water (pH 10, adjusted with ammonia), and solution B: methanol. Chromatography separation was obtained with gradient elution solvent, the gradient elution program was: 0-1.5 min, 98-20% A; 1.5-4 min, 20% A; 4-4.01 min, 20-98% A; 4.01-10 min, 98% A. Monitored ion pairs were m/z 210 - 79 and m/z 299 - 119 for PCr and salidroside in negative ionization mode.

For the separation of Cr, a Hypersil Gold C₁₈ column (150×4.6 mm, 5 μ m, Thermo Scientific, USA) was applied. The mobile phase was solution A: 2 mM ammonium acetate in water (0.4solution B: acetonitrile. Isocratic elution with 30% A was obtained. Monitored ion pairs were m/z 132 - 90 and m/z 135 - 93 for Cr and Cr-d3 in positive ionization mode.

This method was accurate with the intra-day and inter-day precision less than 6%. The lower limit of quantification (LLOQ) for PCr and Cr were 0.5 μ g/mL and 4 μ g/mL, respectively. Measured concentrations

below LLOQ were reported in the dataset.

Population pharmacokinetic model development

A sequential two-step analysis approach to model building was implemented [16]. First, a population pharmacokinetic model of PCr was developed and then parent parameters were fixed to develop the population pharmacokinetic model for Cr. The nonlinear mixed-effects modeling method was applied to establish the population pharmacokinetic model. The PCr and Cr concentrations were fitted using the Phoenix NLME software (version 8.2, Certara, St. Louis, MO) with the first-order conditional estimation-extended least squares (FOCE-ELS) method throughout the model building process. Pharmacokinetic data which were below LLOQ were handled using the M3 method [17]. Model selection criteria were based on goodness-of-fit plots, objective function value (OFV, equal to $-2 \log$ likelihood), akaike information criteria (AIC) and precision of parameter estimates. The complex parent-metabolite joint population pharmacokinetic model was established in a stepwise fashion. First, the base model including PCr and Cr was developed with residual error model and interindividual variability model. After that, covariate effects on base model were investigated to construct the covariate model.

For PCr, structural model was tested either one-compartment or two-compartment PK models. The one-compartment model parameters included volume of distribution (V) and central clearance (CL). For the two-compartment structural model, inter-compartmental clearance (Q) and volume of the second compartment (V2) were included. The structural model for Cr was also tested. The fraction (F_m) of PCr metabolized to Cr was fixed so as to avoid identifiability problem and the volumes of the compartment for Cr was estimated. A published literature reported that a large amount of PCr was metabolized as Cr in animals after intravenous injection of exogenous PCr, and the conversion rate was about three-quarters [10]. In this study, according to the references and the characteristics of drug concentration-time curves of PCr and Cr, the F_m of PCr converted to Cr was assumed to be 0.75. Because of the existence of endogenous Cr which was detected at each of the pre-dose sample, a parameter of the baseline of endogenous Cr levels was added. Allometric scaling based on bodyweight (BW) was applied to the PK parameters. An allometric power model was used with power exponents fixed at 0.75 for clearances and 1.0 for volumes of distribution, as described in the following equations [18, 19]:

$$CL_i = \theta_{CL} \times (BW_i/20)^{0.75} (1)$$

$$V_i = \theta_V \times (BW_i/20)^1 (2)$$

In this expression, CL_i and V_i are the typical clearance and central volume of distribution for an individual i with bodyweight BW_i while θ_{CL} and θ_V are the respective parameter values for a subject with a bodyweight of 20 kilogram.

The inter-individual variability (η) of pharmacokinetic parameters was assumed to follow a log-normal distribution with a mean of 0 and a variance of ω^2 . Exponential formula was applied to account for IIV (Equation 3).

$$P_{ij} = P_j \times e^{\eta_{ij}} (3)$$

where P_j and P_{ij} represent the typical value of j th population parameter and i th individual's j th parameter.

Proportional error model (Equation 4), additive error model (Equation 5), additive and proportional error model (Equation 6), and power error model (Equation 7) were evaluated to describe the residual error.

$$C_{ij} = IPRED_{ij} \times (1 + \varepsilon_{ij}) (4)$$

$$C_{ij} = IPRED_{ij} + \varepsilon_{ij} (5)$$

$$C_{ij} = IPRED_{ij} \times (1 + \varepsilon_{ij,1}) + \varepsilon_{ij,2} (6)$$

$$C_{ij} = IPRED_{ij} + IPRED_{ij}^{0.5} \times \varepsilon_{ij} (7)$$

where C_{ij} was the observation concentration of i th individual at the j th sampling point and $IPRED_{ij}$ was the individual prediction value. The residual error (ϵ) is normally distributed with a mean of 0 and a variance of σ^2 .

The impact of covariates on pharmacokinetic parameters was evaluated. The relationship between covariates and IIV for pharmacokinetic parameters were investigated graphically ahead of covariate assessment. In this dataset, both categorical variables (gender) and continuous variables (height, BW, age, disease duration, WBC, RBC, hemoglobin, PLT, NEUT, LYMPH, MONO, EO, BASO, TP, ALB, ALP, AST, ALT, TBIL, DBIL, urea, creatinine, UA, CK, CK-MB, LDH, HBDH, HSTN-I, GFR) were tested. Categorical covariates were included in the population model with the use of indicator variables and the impact of the categorical covariates on each parameter was tested using power function. Continuous covariates were centered at their median values, and the impacts of each covariate on parameters were evaluated using power functions. The stepwise forward addition and backward elimination were applied to develop the covariate model. In the forward addition, a covariate was retained if it resulting in a reduction the $OFV > 6.64$ ($P < 0.01$, $df = 1$). In the backward elimination, each covariate was left out of the full model built by forward addition one at a time. A covariate was retained if the elimination of the covariate lead to an increase of $OFV > 10.83$ ($P < 0.001$, $df = 1$).

Goodness-of-fit and model evaluation

To describe the adequacy of the final population pharmacokinetic model, goodness-of-fit plots including observations versus population predictions, observations versus individual predictions, conditional weighted residuals (CWRES) versus population predictions, CWRES versus time were assessed. To evaluate the stability of final pharmacokinetic model, a bootstrap resampling procedure was performed. A total of 1000 bootstrap datasets were generated by random sampling with replacement and the pharmacokinetic parameters were re-estimated using the final population model. The median parameter value and their 95% confidence intervals (95% CIs) from bootstrap estimates were compared with the estimates of the final model. In addition, a visual predictive check (VPC) was used to assess the predictive ability of the final model. A total of 1000 simulations of the final population pharmacokinetic model were performed. The VPC graphically showed the observations and different percentiles of simulated concentrations (5th, median, and 95th percentiles).

Simulation

The final PCr and Cr joint population pharmacokinetic model was used to simulate different regimens for pediatric patients with myocarditis. Pediatric patients were divided into different subgroups in accordance with age (Group1: 28 days \sim < 1 year old; Group2: 1 \sim < 6 years old; Group3: 6 \sim < 18 years old). Dose followed the dosage guideline of this trial (Group1: 0.5 g, Group2: 1 g, Group3: 2 g). Monte Carlo simulations were carried out to find the concentration curve under continuous drug administration. The simulated regimens are as follows:

Regimen1: the drug was intravenous administered once a day with infusion time of 30 min for each infusion. The administration interval was 24 h and drug was administered continuously for 4 days.

Regimen2: the drug was intravenous administered twice a day with infusion time of 30 min for each infusion. The administration interval was 12 h and drug was administered continuously for 4 days.

Regimen3: the drug was intravenous administered twice a day with infusion time of 300 min for each infusion. The administration interval was 12 h and drug was administered continuously for 4 days.

Regimen4: the drug was intravenous administered twice a day with infusion time of 600 min for each infusion. The administration interval was 12 h and drug was administered continuously for 4 days.

Results

Patient characteristics

A total of 100 pediatric patients (56 males and 44 females) with a median age of 5.78 years old (range from 0.38 to 16.45 years old) and a median BW of 20.4 kg (range from 7.9 to 86 kg) were enrolled in this study. Participant demographic characteristics are shown in **Table 1** . A total of 997 plasma concentrations (498 for PCr and 499 for Cr) were included in the analysis. Approximately 48.7% of the PCr concentrations were below LLOQ and were handled using the M3 method [17]. All the Cr concentrations were above LLOQ. The baseline covariates information in this data set are shown in **Supplemental Material 1** .

Population pharmacokinetic model

Based on the goodness-of-fit and obtained OFV and AIC, a four-compartment chain model with first-order elimination adequately described the PCr and Cr data. The schematic diagram is shown in **Figure 1** . The disposition of PCr in blood was characterized by a two-compartment model (compartment 1 and 2) which includes central volume of distribution (V_{cPCr}), peripheral volume of distribution (V_{pPCr}), central clearance (CL_{PCr}) and inter-compartmental clearance (Q_{PCr}). The parent PCr was converted into metabolite Cr. The disposition of Cr in blood was described using another two-compartment model (compartment 3 and 4) including central volume of distribution (V_{cCr}), peripheral volume of distribution (V_{pCr}), central clearance (CL_{Cr}) and inter-compartmental clearance (Q_{Cr}). The fraction (F_m) of PCr metabolized to Cr was fixed to 0.75 and it was assumed that 75 percent PCr was eliminated via metabolic conversion to Cr. Besides, another parameter of the baseline endogenous Cr (baseCr) was incorporated into the model to describe this basal value. The following are the differential functions to describe the process:

$$\frac{dA_1}{dt} = A_0 - \frac{CL_{PCr}}{V_{cPCr}} \times A_1 + \frac{Q_{PCr}}{V_{pPCr}} \times A_2 - \frac{Q_{PCr}}{V_{cPCr}} \times A_1 \quad (8)$$

$$\frac{dA_2}{dt} = -\frac{Q_{PCr}}{V_{pPCr}} \times A_2 + \frac{Q_{PCr}}{V_{cPCr}} \times A_1 \quad (9)$$

$$\frac{dA_3}{dt} = \frac{CL_{PCr}}{V_{cPCr}} \times A_1 \times F_m - \frac{CL_{Cr}}{V_{cCr}} \times A_3 + \frac{Q_{Cr}}{V_{pCr}} \times A_4 - \frac{Q_{Cr}}{V_{cCr}} \times A_3 \quad (10)$$

$$\frac{dA_4}{dt} = -\frac{Q_{Cr}}{V_{pCr}} \times A_4 + \frac{Q_{Cr}}{V_{cCr}} \times A_3 \quad (11)$$

$$CobsPCr = \frac{A_1}{V_{cPCr}} \quad (12)$$

$$CobsCr = \frac{A_3}{V_{cCr}} + baseCr \quad (13)$$

A_1 and A_2 are the PCr amount in the central and peripheral compartments, respectively. A_3 and A_4 are the Cr amount in the central and peripheral compartments, respectively. A_0 represents the administration rate of creatine phosphate sodium in blood. F_m represents the fraction of PCr metabolized to Cr. CobsPCr and CobsCr are the observed drug concentration of PCr and Cr in the central compartment (plasma concentration), respectively. The definition of the other parameters (V_{cPCr} , V_{pPCr} , CL_{PCr} , Q_{PCr} , V_{cCr} , V_{pCr} , CL_{Cr} , Q_{Cr} , baseCr) can be found in **Figure 1** .

The interindividual variability was estimated for CL_{PCr} , V_{cCr} , V_{pCr} , CL_{Cr} , and baseCr. The proportional error accounted for the residual error model of both PCr and Cr observations. Finally, the OFV of the base model was 6785.535. According to the criteria of forward inclusion and backward exclusion, covariate GFR was identified and included in the final population pharmacokinetic model. The incorporation of covariate markedly decreased the OFV from 6785.535 to 6773.0502 ($\Delta OFV = -12.4848$). In the final model, GFR had a positive significant influence on CL_{Cr} and their relationship was described by the following

$$CL_{Cr} \text{ (L/min)} = 0.0825 \times (BW/20)^{0.75} \times (GFR/127.78)^{0.311} \times e^{\eta_{CL_{Cr}}} \quad (14)$$

In equation (14), 0.0825 L/min is the typical value of CL_{Cr} , 20 kg is the median value of BW, 127.78 mL/min/1.73m² is the median value of GFR and 0.311 is the correlation coefficient between BW and CL_{Cr} . The estimated values of the parameters of the final model, their relative standard error (RSE) and interindividual variability are summarized in **Table 2** . All parameters were estimated with acceptable precision with RSE of estimates < 30%. The shrinkage in random IIV estimates for CL_{PCr} , V_{cCr} , V_{pCr} , CL_{Cr} , and baseCr were 3.93%, 10.3%, 22.6%, 5.22% and 1.04% respectively.

Goodness-of-fit and model evaluation

The goodness-of-fit plots for both PCr and Cr observations of the final model are shown in **Figure 2**. The plots for CWRES (PCr and Cr) versus time or population predictions are shown in Figures 2A and 2B which were used to detect any misspecifications in the model. The CWRES of the final pharmacokinetic model distributed around the line $y = 0$ indicating no apparent systematic bias were observed. Scatter plots of observation (PCr and Cr concentrations) versus population or individual predictions are shown in Figures 2C and 2D, and the solid lines are the unity. The data points distributed evenly around the line of identity in the final model (Figure2C). These diagnostic plots suggested a good fit of the proposed final model to the data.

The evaluation of 1000 bootstrap runs with a success rate 98.3% (983 out of 1000 resampling datasets were successful in optimization) showed an acceptable stability of the final population pharmacokinetic model. Bootstrap results of median parameter values and 95% CIs are listed in **Table 2**. The median values are similar to the final parameter estimates and 95% CIs are closed to the values obtained during final data fitting. The VPC results (PCr and Cr) are shown in **Figure 3**. In the VPC plot, 90% prediction interval (90% PI) is the area between predicted 5th and 95th percentiles (black dashed lines) and the majority of actual observations fell within the 90% PI. The predicted 5th 50th and 95th percentiles (black lines) are closed with the observed 5th 50th and 95th percentiles (red lines), respectively. This plot indicated an adequate predictive ability of the final population model.

Simulation

The simulation results showed that the PCr had no accumulation in vivo. Under the regimen1 and 2, the PCr was basically eliminated within 3 hours (the concentration of 50th quantile of 1000 simulations was less than $0.1 \mu\text{mol/L}$). Increasing infusion time (regimen3 and 4) could prolong the residence time of PCr in vivo and maintain a certain concentration of PCr. With the infusion of PCr, the concentration of Cr in vivo increased rapidly. In regimen1 and 2, Cr was basically eliminated to the baseline level after 12h (the concentration of 50th quantile in 1000 simulated profiles was similar to the baseline level $67 \mu\text{mol/L}$). The simulation curves are shown in **Supplemental Material 2**.

Discussion

Although the pharmacokinetics of PCr has already been investigated in adults, its pharmacokinetic characteristics in children is unclear and its metabolite Cr was ignored. To the best of our knowledge, this is not only the first PK study of PCr in children but also the first comprehensive population pharmacokinetic model of PCr and its metabolite Cr. In this study, the pharmacokinetic characteristics of PCr and Cr in children were studied by population pharmacokinetic method and the established joint model fitted the concentration data well. This study could be helpful to further understand the PCr and Cr PK characteristics in children and provide reference for pediatric clinical application.

In the base model development process, the structural model of both PCr and Cr were tested with one-compartment model and two-compartment model respectively. The PCr data was best fitted by a two-compartment model which is in accordance with a previous report [10, 11]. The structural model of Cr was best described by a two-compartment model with an estimation of baseline level of Cr level (baseCr).

There is only PCr dose for each subject and Cr was generated by PCr metabolism. The distribution volume of Cr and F_m of PCr metabolized to Cr couldn't be estimated at the same time. It has been reported that large number of PCr were metabolized to Cr in animals after intravenous administration of PCr, and the conversion rate was about three-quarters [10]. In the concentration–time plots (**Supplemental Material 3**), Cr concentration increased rapidly after PCr infusion. In our study, we were more interested in knowing the distribution of Cr in children. Therefore, the apparent distribution volume of Cr was estimated and the fraction of PCr metabolized to Cr was fixed so as to avoid identifiability problem in the model building. There is no evidence that showed the exact ratio fraction of PCr to Cr in humans. The Cr concentration increased rapidly with the infusion of PCr seen in the concentration profiles and a general view is that a

large amount of PCr is metabolized to Cr to provide ATP after PCr injection [5]. In this study, based on the results of animal experiment from the reference [10], the F_m of PCr converted to Cr was assumed to be 0.75. This setting could ensure the estimation the PK parameters of Cr in children and it didn't affect the estimation of PCr parameters. To compare the estimation results of different fraction assumptions, we developed a model based on the fraction fixed 1 and the estimation results showed PCr parameters did not change much.

BW was incorporated in the base model with an allometric exponent of 0.75 for the clearance parameters and 1 for the volume terms which result in a large decrease in OFV. The addition of allometric scaling made the base model more stable and accelerated the speed of modeling. In this study, to find more factors that affect the in vivo behavior of the PCr and Cr as much as possible, a large amount of information of study sample were collected as covariates. After forward inclusion and backward elimination, GFR was identified as key covariates to the clearance of Cr. The influence of GFR on CL_{Cr} was estimated with exponent of 0.311, which means high level of GFR level lead to increase of Cr clearance. As GFR increased by 100%, Cr clearance increased by 24%.

The final PCr and Cr model was evaluated by bootstrap and VPC method, respectively. Results showed that the established model had good stability and predictability. The parameters estimated by the final model showed that distribution volume of the PCr central compartment (V_{cPCr}) was 8.22 L, distribution volume of the PCr peripheral compartment (V_{pPCr}) was 3.07 L, total distribution volume was 11.29 L, and the clearance was 1.33 L/min in children with 20 kg. The distribution volume of the Cr central compartment (V_{cCr}) was 2.39 L, distribution volume of the Cr peripheral compartment (V_{pCr}) was 2.9 L, and the clearance was 0.0825 L/min in children with 20 kg. The V_{pCr} is larger than V_{cCr} , suggesting that Cr can be widely distributed in muscle and other tissues. This study first reported the distribution characteristics of Cr in children under the F_m set to 0.75. The typical value of Cr base value (baseCr) is 66.6 $\mu\text{mol/L}$, which is about 8.73 mg/L, basically consistent with the normal content in human body (7-13 mg/L) [20]. The evaluated model was applied to simulate different regimens for subgroups with different age. The simulation results suggested that PCr did not accumulate in vivo.

In conclusion, the joint population pharmacokinetic model for PCr and its metabolite Cr in pediatric patients was successfully developed for the first time. The model adequately described the pharmacokinetics of both parent drug and metabolite with individual predicted value close to the measured value. This model may be helpful for pediatric clinical application of phosphocreatine.

Acknowledgements

The authors acknowledge the support of Haerbin laibotong pharmaceutical co. LTD for the clinical trial from which the Phosphocreatine and Creatine pharmacokinetic data were derived.

Competing Interests

The authors declare no conflicts of interest.

Contributors

All authors contributed to the design and implementation of the study. L.B.Z., Y.Y. and X.L.W. designed the study. N.S. and H.H. acquired the data. M.Z., Y.Z. and H.H. analyzed the data and develop the pharmacokinetic model. H.H. wrote the manuscript and L.B.Z., Y.Y. and X.L.W. revised it.

Funding

This work was supported in part by grants from National Science and Technology Major Project for Major New Drugs Innovation and Development (2017ZX09304029 and 2018ZX09721003).

Data Availability Statement

The data for this article are not publicly available because of privacy and ethical restrictions. Requests to access the data should be directed to corresponding author.

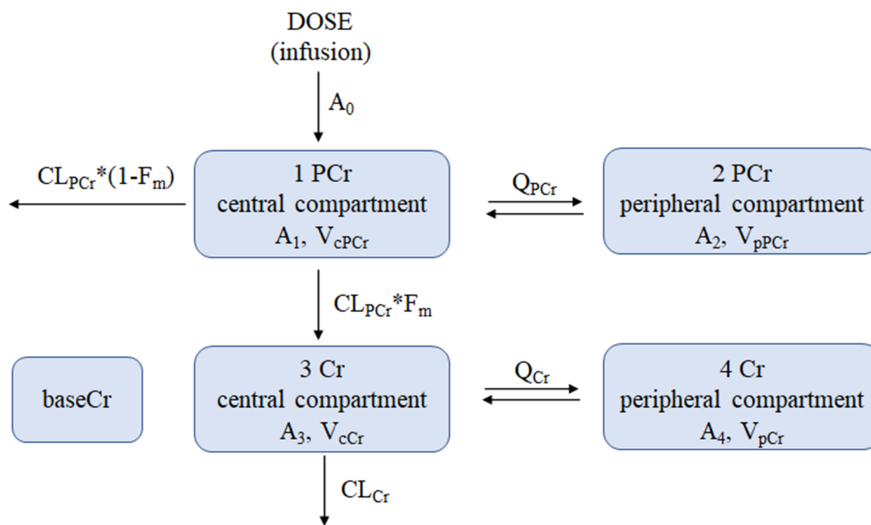
References

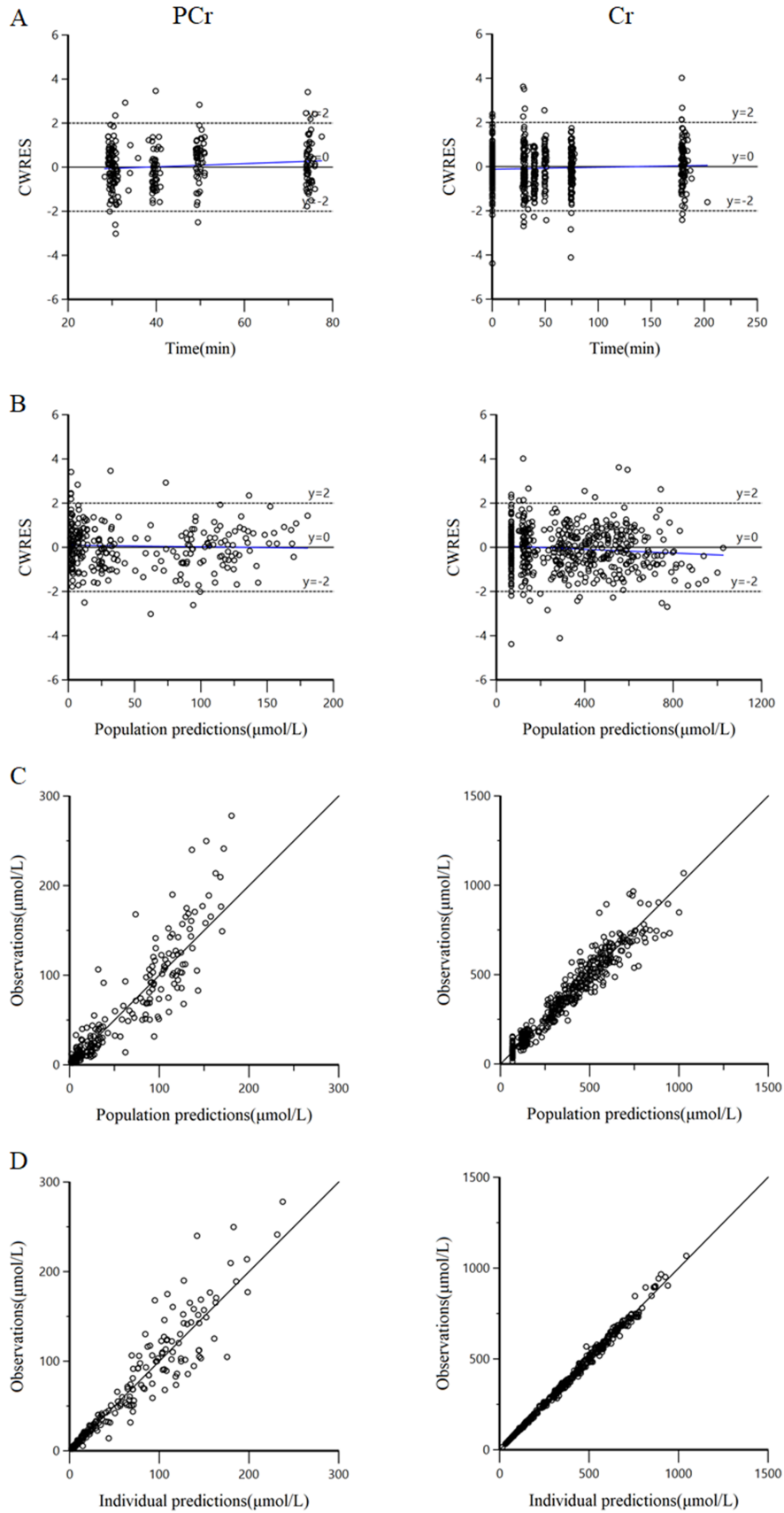
- 1 Bejiqi R, Retkocer R, Maloku A, Mustafa A, Bejiqi H, Bejiqi R. The Diagnostic and Clinical Approach to Pediatric Myocarditis: A Review of the Current Literature. *Open Access Maced J Med Sci* 2019; 7: 162-173.
- 2 Niu L, An XJ, Tian J, Wang Y. 124 cases of clinical analysis of children with viral myocarditis. *Eur Rev Med Pharmacol Sci* 2015; 19: 2856-9.
- 3 Gabr RE, El-Sharkawy AM, Schär M, Weiss RG, Bottomley PA. High-energy phosphate transfer in human muscle: diffusion of phosphocreatine. *Am J Physiol Cell Physiol* 2011; 301: 234-41.
- 4 Wallimann T, Tokarska-Schlattner M, Schlattner U. The creatine kinase system and pleiotropic effects of creatine. *Amino Acids* 2011; 40: 1271-96.
- 5 Neubauer S. The failing heart—an engine out of fuel. *N Engl J Med* 2007; 356: 1140-51.
- 6 Kôrge P, Silber ML, Gollnick PD. Effect of creatine phosphate on the contractile activity in acutely failing rat heart. *Cardiologia* 1998; 43: 1345-54.
- 7 Saks VA, Dzhalishvili IV, Konorev EA, Strumia E. Molecular and cellular aspects of the cardioprotective mechanism of phosphocreatine. *Biokhimiia* 1992; 57: 1763-84.
- 8 Sharov VG, Afonskaya NI, Ruda MY, Cherpachenko NM, Pozin EYa, Markosyan RA, *et al* . Protection of ischemic myocardium by exogenous phosphocreatine (neoton): pharmacokinetics of phosphocreatine, reduction of infarct size, stabilization of sarcolemma of ischemic cardiomyocytes, and antithrombotic action. *Biochem Med Metab Biol* 1986; 35: 101-14.
- 9 Strumia E, Pelliccia F, D'Ambrosio G. Creatine phosphate: pharmacological and clinical perspectives. *Adv Ther* 2012; 29: 99-123.
- 10 Xu L, Wang CY, Lv L, Liu KX, Sun HJ, Han GZ. Pharmacokinetics of phosphocreatine and its active metabolite creatine in the mouse plasma and myocardium. *Pharmacol Rep* 2014; 66: 908-14.
- 11 Lorenzi E, Piacenza G, Strumia E, Borgoglio R. Pharmacokinetics of phosphocreatine following intravenous administration in humans and effect on blood levels of ATP. *Cardiologia* 1987; 32: 1031-4.
- 12 Afonskaia NI, Shepeleva II, Aniukhovskii EP, Samarenko MB, Makhotina LA. Pharmacokinetics of phosphocreatine in the blood serum of man, dogs and rabbits. *Biull Eksp Biol Med* 1985; 100: 591-3.
- 13 Schwartz GJ, Muñoz A, Schneider MF, Mak RH, Kaskel F, Warady BA. New equations to estimate GFR in children with CKD. *J Am Soc Nephrol* 2009; 20: 629-37.
- 14 Schwartz GJ, Haycock GB, Edelmann CM Jr, Spitzer A. A simple estimate of glomerular filtration rate in children derived from body length and plasma creatinine. *Pediatrics* 1976; 58: 259-63.
- 15 Sun N, Li Q, Zhao L, He H, Zhang M, Wang X. Simultaneous quantitative analysis of phosphocreatine, creatine and creatinine in plasma of children by HPLC-MS/MS method: Application to a pharmacokinetic study in children with viral myocarditis. *Biomed Chromatogr* 2019; 33: e4558.
- 16 Patel YT, Daryani VM, Patel P, Zhou D, Fangusaro J, Carlile DJ. Population Pharmacokinetics of Selumetinib and Its Metabolite N-desmethyl-selumetinib in Adult Patients With Advanced Solid Tumors and Children With Low-Grade Gliomas. *CPT Pharmacometrics Syst Pharmacol* 2017; 6: 305-314.
- 17 Beal SL. Ways to fit a PK model with some data below the quantification limit. *J Pharmacokinetic Pharmacodyn* 2001; 28: 481-504.

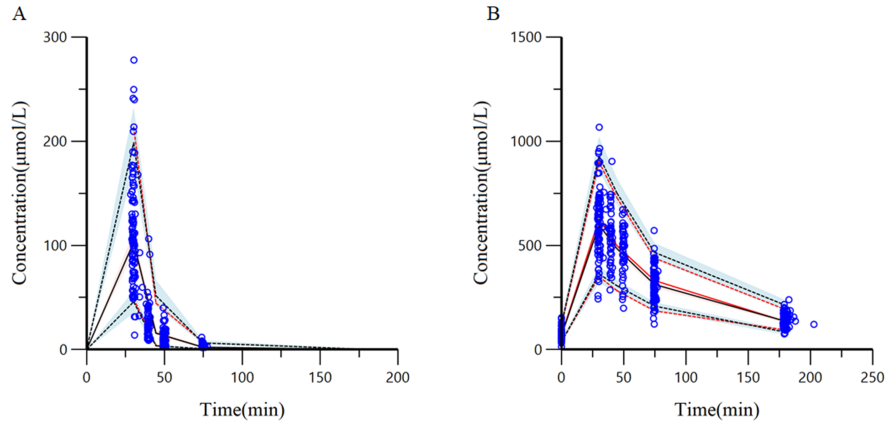
18 Hazendonk H, Fijnvandraat K, Lock J, Driessens M, van der Meer F, Meijer K, *et al* . A population pharmacokinetic model for perioperative dosing of factor VIII in hemophilia A patients. *Haematologica* 2016; 101: 1159-1169.

19 Björkman S, Folkesson A, Jönsson S. Pharmacokinetics and dose requirements of factor VIII over the age range 3-74 years: a population analysis based on 50 patients with long-term prophylactic treatment for haemophilia A. *Eur J Clin Pharmacol* 2009; 65: 989-98.

20 Persky AM, Brazeau GA, Hochhaus G. Pharmacokinetics of the dietary supplement creatine. *Clin Pharmacokinetics* 2003; 42: 557-574.







Hosted file

Tables.docx available at <https://authorea.com/users/324471/articles/452645-population-pharmacokinetics-of-phosphocreatine-and-its-metabolite-creatine-in-children-with-myocarditis>

Hosted file

Supplemental Material 1.docx available at <https://authorea.com/users/324471/articles/452645-population-pharmacokinetics-of-phosphocreatine-and-its-metabolite-creatine-in-children-with-myocarditis>

